2

Electrostatically generated nanofibres for wearable electronics

F R A N K K . K O , A F A F E L - A U F Y and H O A L A M
Drexel University, USA

A L A N G . M A C D I A R M I D
University of Pennsylvania, USA

2.1 Introduction

Wearable electronics are electronic devices constantly worn by a person as unobstructively as clothing to provide intelligent assistance that augments memory, intellect, creativity, communication and physical senses.[1,2] Wearable electronics can be worn internally as implantable devices such as pacemakers and neuroprosthetics. Wearable electronics may be worn externally in the form of a ring, a badge, a wristwatch, eyeglasses, jewellery, shoes or clothing. The key considerations for wearable electronics are that they have to be robust, small, consume a small amount of power, and be comfortable to wear. Wearable electronics can function as sensors or as computers that consist of input, output and a motherboard made up of transistors and various interconnections. The wearable computer must be powered by lightweight batteries or fuel cells and must not be much of an additional burden to the wearer. Accordingly, the favourable ingredients for wearable electronics are lightweight, flexible and conductive materials. Conductive materials in fibrous form such as yarns and fabrics are preferred candidates for wearable electronics by serving as interconnects, functional devices and sensors.

Currently, most of the commercially available conductive yarns comprise a blend of non-conductive polymers with conductive particles such as carbon black, metallic particles, blends of polymeric fibres and continuous stainless steel fibres, stainless steel spun fibres and metal-clad aramid fibres.[3] Conductive yarns containing metallic components are prone to damage owing to excessive exposure to moisture and continuous fatigue during wearing and washing. The high stiffness of the metallic wires reduces the flexibility of the fabric, causing discomfort and restricting the mobility of the wearer. Commonly, the wearable electronic device is produced as a separate unit that can be attached to the garment. This allows the device to be removed from the clothes before washing, which is not convenient in

Table 2.1 Commercially available conductive yarns

Thread type	Conductivity (S cm^{-1})
BK 50/2 – Bekaert fibre technologies (steel/polyester spun yarn)	50
Bekintex – Bekaert fibre (continuous cold drawn stainless steel fibres)	1
Bekintex 15/2 – Bekaert fibre (stainless spun fibres)	1
VN 140 nyl/35 × 3 (nylon core wrapped with continuous stainless steel wires)	10
Aracon – DuPont (metal clad aramid fibre) Core: Kevlar Cladding metals: Ag, Ni, Cu, Au, Sn	0.001

some cases. Another method is to integrate the conductive yarns into a base fabric by means of embroidering, weaving, or knitting to generate a circuit pattern. This technique has recently been studied in wearable electronics and wearable computers.[3] Some of the commercially available conductive yarns, along with a brief description and their approximate resistance per unit length, are listed in Table 2.1. These fibres are available in diameters ranging from 100 μm to 12 μm.

The shortcomings of metal-based yarns can be overcome by the use of intrinsically conductive polymers (ICPs) or by a combination of ICPs with non-conductive polymers. ICPs, also known as synthetic metals, are organic polymers that possess the electrical, electronic, magnetic and optical properties of a metal, while retaining mechanical properties and processability. The properties of ICPs are intrinsic to a 'doped' form of the polymer.[4] Polymer-based devices are expected to have the combined advantages of low cost, control of material characteristics and flexible chemistry. Some ICP polymers are listed in Table 2.2, with polyacetylene, poly(3,4-ethylenedioxyphiothene)/poly(styrenesulphonate) (PEDT) and polyaniline (PANi) being the most commercially available and most extensively studied. They are being used in a wide range of applications, from actuators to rechargeable batteries.[3–6] These polymers and their blends are excellent candidates for wearable electronics because of their potential in the formation of fibres. One major concern with ICPs is their current-carrying capability over a long distance. The commercially available ICP fibres tend to be large and less flexible than textile fibres.

In order to improve the conductivity and other functional properties of wearable electronics, we are dedicated to exploring the potential use of nanofibres and nanofibre-based structures as wearable electronics. A significant reduction in the diameter of the fibres is expected to increase their flexibility greatly. The strength of the fibres and of the fibrous assemblies is also expected to increase. Owing to the

Table 2.2 Conductivity of ICPs

Polymer	Approx. conductivity (S cm^{-1})	Polymer	Approx. conductivity (S cm^{-1})
Polyacetylene	10 000[a]	Polythienylenevinylene	2700[a]
Polypyrrole	500–7500	Polyphenylene	1000
Polythiophene	1000	Polyisothianaphthene	50
Poly(3-alkylthiophene)	1000–10 000[a]	Polyazulene	1
Polyphenylene sulphide	500	Polyfuran	100
Polyphenylenevinylene	10 000[a]	Polyaniline	200[a]

[a] Conductivity of oriented polymer.

effect of confinement, unusual properties of current conduction are expected to emerge when the size of the fibres is reduced below a certain critical thickness/ diameter to the nanoscale.[7, 8] Several processes can be used that have the potential to make fibres in the nanoscale. These processes include the template method,[9] the island in the sea technology[10] and the electrostatic spinning process. Of these, the electrostatic spinning process is preferred because of its simplicity and its potential to scale into a continuous process. The electrospinning process allows the nanofibres (diameter less than 100 nm) of organic polymers to be controllably and reproducibly fabricated such that, in one given preparation, all fibres will have a diameter of less than 100 nm. The objective of this chapter is to introduce an electrostatic spinning process for the formation of nanofibres of pure electronic polymers (in their semiconducting and metallic regimes) and/or their blends in conventional organic polymers for the purpose of ascertaining their applicability in the fabrication of nanoelectronic devices for wearable electronics.

2.2   Electrospinning process

2.2.1   Background

The electrostatic generation of ultrafine fibres, a process called electrospinning, has been practised since the 1930s.[11] This technique has been rediscovered for applications such as high-performance filters[12, 13] and for scaffolds in tissue engineering[14] that utilise the high surface area (10 m^2 g^{-1}) unique to these fibres. In this non-mechanical, electrostatic technique, a high electric field is generated between a polymer fluid (contained in a glass syringe with a capillary tip) and a metallic collection screen. When the voltage reaches a critical value, the charge overcomes the surface tension on the deformed drop of the suspended polymer solution that is formed on the tip of the syringe, and a jet is produced. During its passage to the collection screen, the electrically charged jet undergoes a series of electrically induced bending instabilities that results in the hyperstretching of the
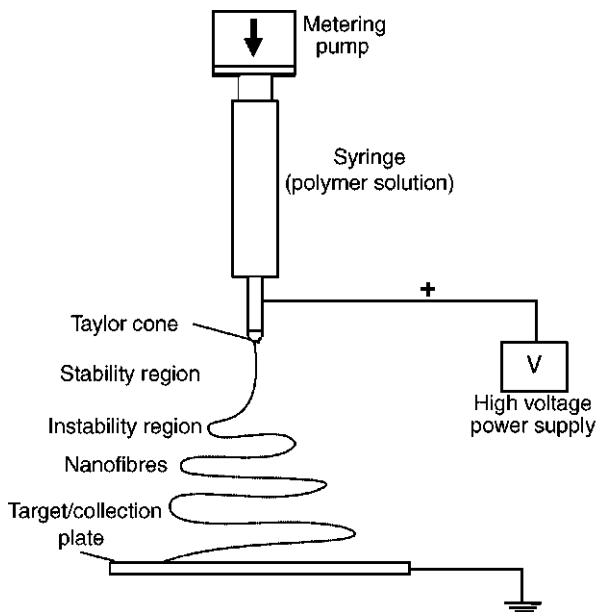
2.1 Schematic of the electrospinning process.

jet. This stretching process is accompanied by rapid evaporation of the solvent molecules that reduces the diameter of the jet to a cone-shaped volume called the envelope cone. The dry fibres are accumulated on the surface of the collection screen, resulting in a non-woven mesh of fibres with diameters between nanometres and micrometres. The process can be adjusted to control the diameter of the fibre by varying the strength of the electrical field and concentration of the polymer solution, while the duration of electrospinning controls the thickness of the deposition of fibres.[11] A schematic drawing of the electrospinning process is shown in Fig. 2.1. Considering the fact that the rate of electrochemical reactions is proportional to the surface area of the electrode, it is of interest to explore the merits of the high surface to volume ratio of electrospun fibres in order to develop porous polymeric electrodes. Reneker and Chun[15] have reported that polyaniline fibres can be successfully electrospun from sulphuric acid into a coagulation bath. Another way of producing electrically conductive nanofibres is by the pyrolysis of electrospun polyacrylonitrile nanofibres into carbon nanofibres.

2.2.2   Controlling the diameter of the fibre

In order to generate fibres in the nanoscale consistently and reproducibly, it is important to understand the parameters affecting the diameter of the fibres by the electrospinning process. Although the process of electrospinning has been known for over half a century, current understanding of the process and those parameters

is very limited. Many processing parameters influence the spinnability and physical properties of nanofibres, including the strength of the electric field, the concentration of the polymers, spinning distance, viscosity of the polymer, and so forth.[16] Experimental evidence has shown that the diameter of the fibre produced by electrospinning is influenced by the concentration of the polymer and by molecular conformation.[17] To establish a processing index for controlling the diameter of fibres, the Berry number (*Be*), a dimensionless parameter,[18] was used:

$$Be = [\eta]*C$$

where $[\eta]$ is the intrinsic viscosity of the polymer and the ratio of the specific viscosity to the concentration at an infinite dilution, and *C* is the concentration of the polymer solution. Intrinsic viscosity is also closely related to the molecular weight of the polymer. It has been found that the degree of the entanglement of polymer chains in a solution can be described by *Be*.[18] In very diluted solutions, when the *Be* is less than unity, the molecules of the polymer are sparsely distributed in the solution. There is a low probability of individual molecules becoming entangled in each other. At a *Be* of greater than unity and as the concentration of the polymers increases, the level of molecular entanglement increases, resulting in more favourable conditions for the formation of fibres.

The relationships between the concentration and the average fibre diameter (AFD) of a poly(L-lactic acid) (PLA) of different molecular weights in chloroform are shown in Fig. 2.2. It can be seen that the diameter of the fibre increases as the concentration of the polymer increases. The diameter of the fibre increases at a greater rate at higher molecular weights. Accordingly, one can tailor the diameter of the fibre through the proper selection of polymer molecular weight and polymer concentration.

Expressing the diameter of a fibre as a function of *Be*, as shown in Fig. 2.3, a pattern emerges indicating four regions of *Be*–diameter relationships. Region I, where *Be* < 1, is characterised by a very diluted polymer solution with molecular chains that barely touch each other. This makes it almost impossible to form fibres by the electrospinning of such a solution, since the chains are not entangled enough to form a continuous fibre and the effect of surface tension will make the extended conformation of a single molecule unstable. As a result, only polymer droplets are formed. In region II, where 1 < *Be* < 3, AFD increases slowly with *Be* from ~100 to ~500 nm. In this region, the degree of molecular entanglement is just sufficient for fibres to form. The coiled macromolecules of the dissolved polymer are transformed by the elongational flow of the polymer jet into oriented molecular assemblies with some level of inter- and intra-molecular entanglement. These entangled networks persist as the fibre solidifies. In this region, some bead formations are observed as a result of the relaxation of the polymers and the effect of surface tension. In region III, where 3 < *Be* < 4, AFD increases rapidly with *Be*, from ~1700 to ~2800 nm. In this region the entanglement of the molecular chain becomes more intensive, contributing to an increase in the viscosity of the polymer. Because of the intense level of molecular entanglement, a stronger
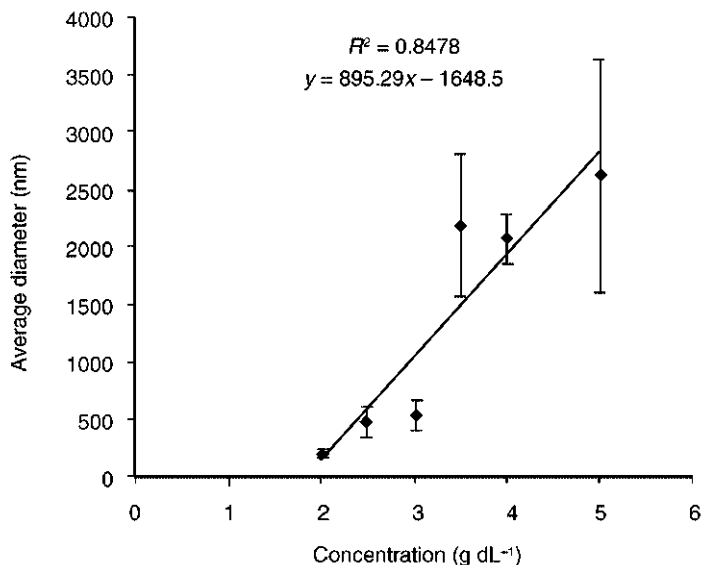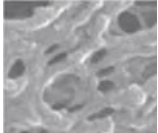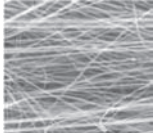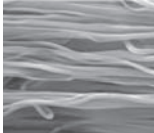
(a)
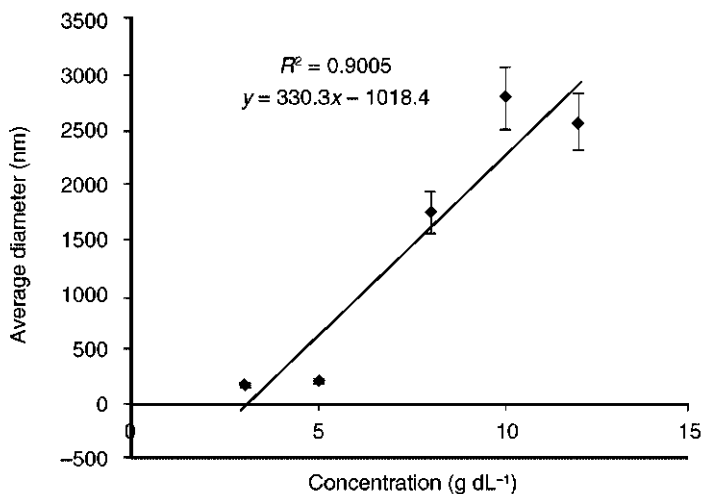
(b)

2.2 Relationships of fibre diameter to concentrations at different molecular weights (MW). (a) MW = 300 000, (b) MW = 200 000.

electric field is needed for fibres to form by electrospinning. In region IV, where *Be* > 4, the AFD is less dependent on *Be*. With a high degree of inter- and intra-molecular chain entanglement, other processing parameters such as the strength of the electric field and spinning distance become dominant factors that affect the diameter of the fibre. A schematic illustration of the four Berry regions is shown in Table 2.3.
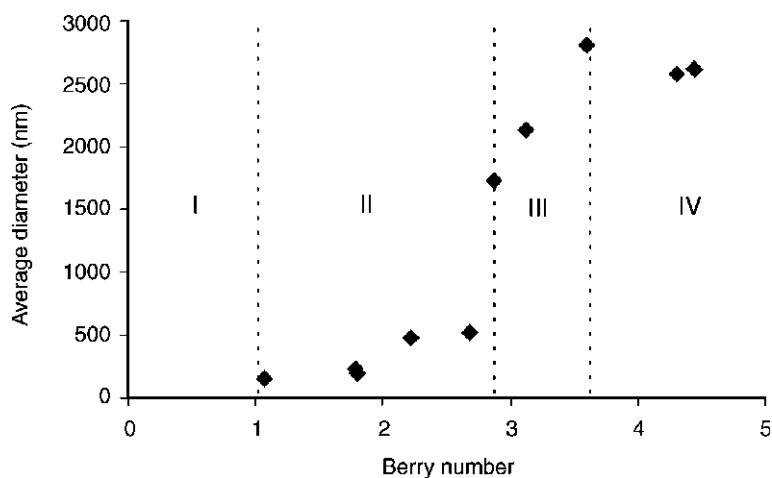
2.3 The relationship between Berry number and average fibre diameter.

Table 2.3 Schematic of polymer chain conformation and fibre morphology corresponding to the four regions of the Berry number

	Region I	Region II	Region III	Region IV
Berry number	$Be < 1$	$1 < Be < 2.7$	$2.7 < Be < 3.6$	$Be > 3.6$
Polymer chain conformation in solution				
Fibre morphology				
Average fibre diameter (nm)	(Only droplets formed)	~100–500	1700–2800	~2500–3000

2.2.3 Formation of yarns and fabrics

Electrospun fibres can be assembled by direct fibre-to-fabric formation to create a non-woven fabric or by the creation of a linear assembly or a yarn. From the yarns, a fabric can be woven, knitted or braided. The linear fibre assemblies can be aligned mechanically or by controlling the electrostatic field. Alternatively, a self-assembled continuous yarn can be formed during electrospinning by properly designing the ground electrode. The rotary electrospinning method for the

formation of aligned nanofibres and the self-assembled continuous yarn process are described here.

Rotary electrospinning

A schematic illustration of rotary electrospinning is shown in Fig. 2.4. The rotary electrospinning system consists of a polymer reservoir, a spinneret, a power supply and a variable speed rotating fibre-collecting disk. As the polymer jet is drawn from the polymer cone, it travels toward the spinning disk. The solidified fibres are deposited on the collector as the solvent evaporates. Since the disk is rotating, the deposited fibres are placed in the direction of the rotation, forming rings of aligned fibres on the disk. The fibres are subsequently collected in batches or continuously collected into well-aligned bundles of yarn.
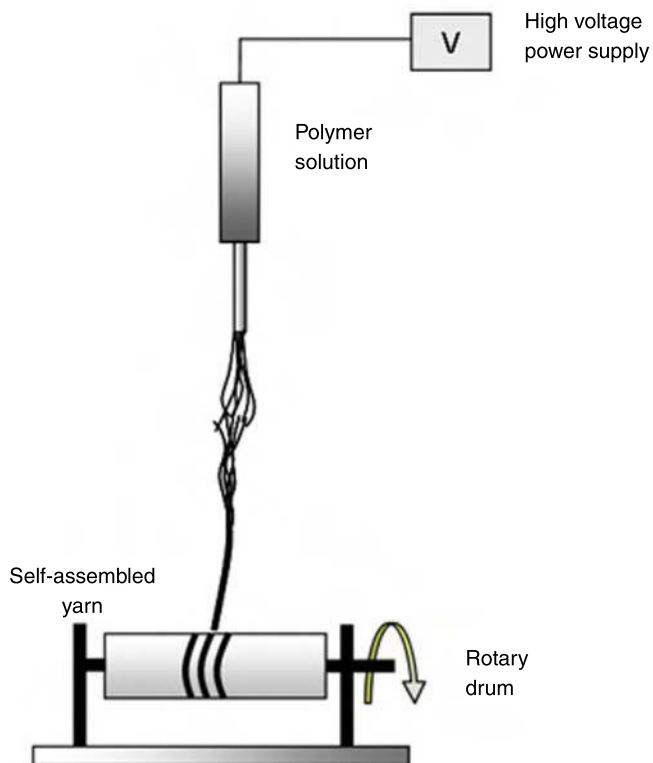
Electrospinning of self-assembled yarn

Self-assembled yarn can be produced in a continuous length with appropriate control of electrospinning parameters and conditions. In this process, the self-assembled yarn is initiated by limiting the footprint of the deposition of fibre into a small area on the target. The fibres are allowed to build on top of each other until a branched tree-like structure is formed. Once a sufficient length of yarn has
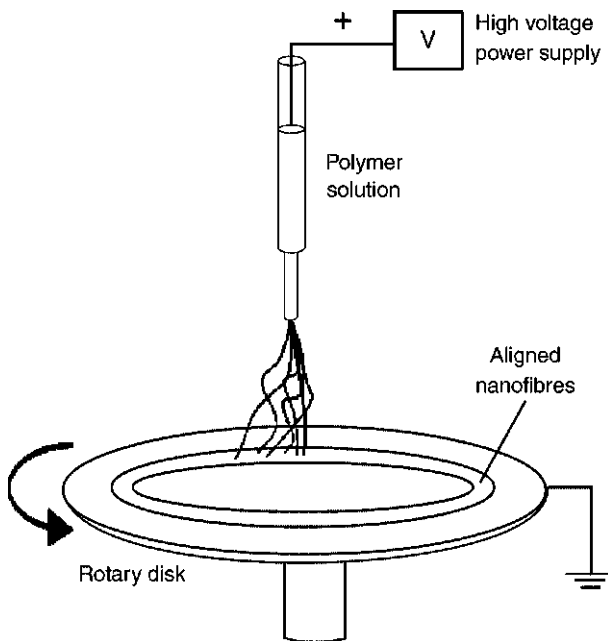
2.4 Schematic drawing of the rotary disk electrospinning process.

2.5 Schematic of the continuous electrospinning of self-assembled yarn.

formed, the accumulated fibres attach themselves to the branches and continue to build up. A device such as a rotating drum can be used to spool up in a continuous length the self-assembled yarn that has been produced, as shown in Fig. 2.5. This method produces bundles of partially aligned nanofibre yarn in a continuous length.

2.3   Electroactive nanofibres

2.3.1   Inherently conductive polymers and blends

ICPs and blends of ICPs with other fibre-forming polymers can be electrospun into linear and planar assemblies. We have previously reported[19] the fabrication of the first conducting polymer fibres (diameter ~950 to 2100 nm) of polyaniline doped with d,l-camphorsulphonic acid (PANi.HCSA) as a blend in polyethylene oxide (PEO). It was discovered that an electronic polymer such as polyaniline, which

might have been expected to be more susceptible to degradation than most conventional organic polymers, survived without observable chemical or physical change following the 25 kV electrospinning–fabrication process in air at room temperature. The fibre diameter morphology of the polymer-blend electrospun fibres was examined using a scanning electron microscope (SEM). According to the SEM micrographs for the different blends of PANi.HCSA/PEO fibres that were investigated, these fibres showed a similar diameter and morphology as the PEO fibres. For example, the SEM micrograph of the non-woven mat of electrospun fibres from a 2 wt% PANi.HCSA/2 wt% PEO solution, shown in Fig. 2.6, revealed that the fibres in the non-woven mat ranged from between 950 nm and 1.9 µm (average fibre diameter, 1.6 µm) and had a generally uniform thickness. Again, the electrospun fibres were distributed randomly in the non-woven mat. From the SEM micrographs of all of the different polyaniline/PEO blends that were electrospun at an electrical field strength of 1 kV cm^{-1}, it appears that the addition of PANi.HCSA to the PEO solution had little effect on the diameter of the electrospun fibre. The PANi.HCSA/PEO electrospun fibres that were produced showed no evidence of birefringence, thus indicating that the polymer chains in the fibre were not oriented with respect to the axis of the fibre.

The conductivity of the electrospun PANi.HCSA/PEO fibres and the cast film on a microscope glass slide was measured using the four-point probe method.[20] The thickness of the non-woven fibre mat and the cast films were measured using a digital micrometer (Mitutoyo) with a resolution of 1 µm. The current was applied between the outer electrodes using a Princeton Analytical Research 363 potentiostat/galvanostat, and the resulting potential drop between the inner electrodes was measured with a Keithley 169 multimeter. Figure 2.7 shows the room temperature conductivity of the PANi.HCSA/PEO electrospun fibres and cast films at various

100 µm
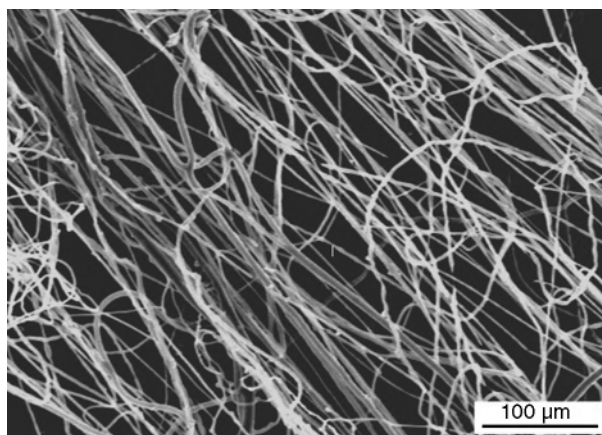
2.6 Nanofibre blend of PANi.HCSA fabricated from 2 wt% PANi.HCSA and 2 wt% PEO in chloroform solution at 25 kV (anode/cathode separation, 25 cm).
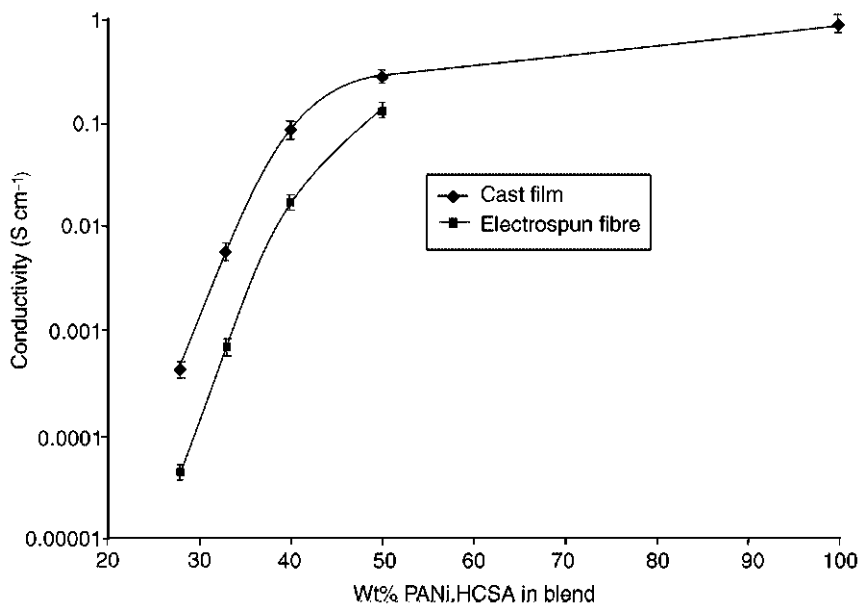
2.7 Electrical conductivity of the PANi.HCSA/PEO blend electrospun fibres and cast films prepared from the same solution (the unit for conductivity on the ordinate is S cm⁻¹ based on a four probe measurement).

ratios of polyaniline and polyethylene oxide in the blend. This graph demonstrates that the conductivity of the electrospun fibres in the non-woven mat is significantly lower than that for a cast film at the same concentration of polyaniline. This is not an unexpected result, as the four-point probe method measures the volume resistivity from which the conductivity can then be calculated and not that of an individual fibre. It must be noted that obtaining the conductivity of the non-woven mat was considerably more difficult than measuring the conductivity of the cast film, owing to the difficulty in obtaining an accurate measurement of thickness on the highly compressible non-woven mat using the micrometer. As can be seen from the SEM micrographs of the electrospun fibres (Fig. 2.6), the non-woven mat is highly porous and therefore the 'fill factor' of the polyaniline fibres is less than that of a cast film. However, it is reasonable to expect that the conductivity of an individual electrospun fibre will be higher than that of the non-woven mat and, in fact, should be approximately equal to the conductivity of the cast film.

Since the submicrometre fibres (500–1600 nm) obtained in our initial work (Fig. 2.6) were not classifiable as true nanofibres, we turned our attention to the consistent and reproducible fabrication of the true nanofibres (diameter <100 nm) of an organic polymer. This was accomplished using an 8 wt% solution of polystyrene (MW 212 400, Aldrich Co) in tetrahydrofuran (THF) (glass pipette orifice, 1.2 mm) at a potential of 20 kV between the anode and cathode, which

were separated by 30 cm. The fibres were collected as a mat on an aluminum target and found by SEM to have the following diameter characteristics: average, 43.1 nm; maximum, 55.0 nm; minimum, 26.9 nm. Other studies involved polystyrene-produced fibres whose diameters were consistently less than 100 nm. For example, another sample of polystyrene had the following fibre diameter characteristics: average, 30.5 nm; maximum, 44.8 nm; minimum, 16.0 nm. It should be noted that these data represent a decrease (of approximately two orders of magnitude) in fibre diameter as compared to those obtained in our earlier studies (Fig. 2.6). It should also be noted that the above 16 nm fibre is ~ 30 polystyrene molecules wide. Dimensions of this size can be expected greatly to affect the kinetics, as well as possibly the thermodynamics, of the polymer. It is also of interest to note that a 16 nm fibre, such as the one mentioned above, lies well within the ~ 4–30 nm range of the diameter of multiwalled carbon nanotubes.[21]

Using a previously observed method for producing polyaniline fibres,[19] we prepared highly conducting sulphuric acid-doped polyaniline fibres (average, 139 nm; maximum, 275 nm; minimum, 96 nm) by placing a ~ 20 wt% solution of polyaniline (Versicon™ Allied Signal) in 98% sulphuric acid in a glass pipette. The tip of the pipette was ~ 3 cm above the surface of a copper cathode immersed in pure water at a potential difference of 5 kV. The fibres collected in or on the surface of the water. As expected, the conductivity of a single fibre was ~ 0.1 S cm^{-1}, since partial de-doping of the fibre occurred in the water cathode.

It is relatively easy to prepare conducting blends of PANi.HCSA in a variety of different conventional polymers such as PEO, polystyrene, polyacrylonitrile, and so forth. For example, ~ 20 wt% blends of PANi.HCSA in polystyrene (MW 114 200) are obtained by electrospinning in a chloroform solution. Their fibre diameter characteristics are: average, 85.8 nm; maximum, 100.0 nm; minimum 72.0 nm. These fibres are sufficiently electrically conductive that their SEMs may be recorded without the necessity of applying a gold coating. Separate, individual nanofibres can be collected and examined if so desired. An appropriate substrate – a glass slide, silicon wafer, or loop of copper wire, etc. – is held between the anode and cathode at a position close to the cathode for a few seconds to collect individual fibres. The current/voltage (*I/V*) curves are given in Fig. 2.8 for a single 419 nm diameter fibre (fibre 1) of a blend of 50 wt% PANi.HCSA, and polyethylene oxide is collected on a silicon wafer coated with a thin layer of SiO$_2$. Two gold electrodes separated by 60.3 μm are deposited on the fibre after its deposition on the substrate. The conductivity (two probes) of fibre 1 (diameter ~ 600 nm) is ~ 10^{-1} S cm^{-1}. The conductivity (two probe) of fibre 2 (diameter ~ 419 nm) is ~ 10^{-1} S cm^{-1}. Non-linear *I/V* curves may be obtained from some polyaniline samples, possibly caused by the presence of defect sites induced by imperfections or impurities in the polyaniline. Such imperfections are expected to be more apparent in thin fibres, since there are fewer molecular pathways by which charge carriers can by-pass the defect sites.

The (reversible) conductivity/temperature relationship between 295 and 77 K
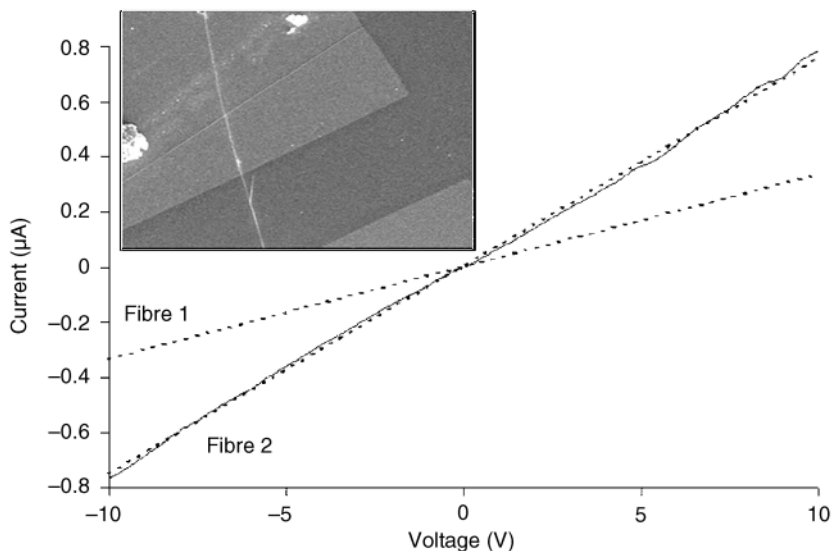
2.8 Current/voltage curves of 50 wt% PANi.HCSA/PEO blend nanofibres. The inset shows a fibre spun from a blend of 50 wt% PANi.HCSA and polyethylene oxide collected on a silicon wafer coated with a thin layer of SiO_2.

for a single 1320 nm fibre containing 72 wt% PANi.HCSA in PEO spun from chloroform solution is given in Fig. 2.9. To minimise the effects of heating, the applied voltage was held constant at 10 mV, at which value the current is very small. The conductivity ($\sim$ 33 S cm^{-1} at 295 K) was unexpectedly large for a blend since the conductivity of a spun film of the pure polymer cast from chloroform solution is only $\sim$ 10^{-1} S cm^{-1}.[22] This suggests that there may be a significant alignment of polymer chains in the fibre.[23]

Poly(3,4-ethylenedioxythiophene)/poly(styrenesulphonate) (Eleflex-2000) and PEDT are popular electronic polymers used for electronic components such as light-emitting diodes (LED). It has been demonstrated in our laboratory that PEDT can be mixed with various polymers to form conductive nanofibres by adding an appropriate amount of PEDT as a percentage of weight to a solvent such as *N,N*-dimethylformamide (DMF) and stirred magnetically for 10–15 minutes. The mixture is then added to a polymer such as polyacrylonitrile (PAN) and stirred for an additional 20 minutes at 60°C.[24]

Figure 2.10 shows an SEM image of the PEDT/PAN electrospun fibres from a combination of 20 wt% PEDT and 8 wt% PAN. A high level of fibre alignment was achieved by the yarn-self-assembly process during electrospinning.
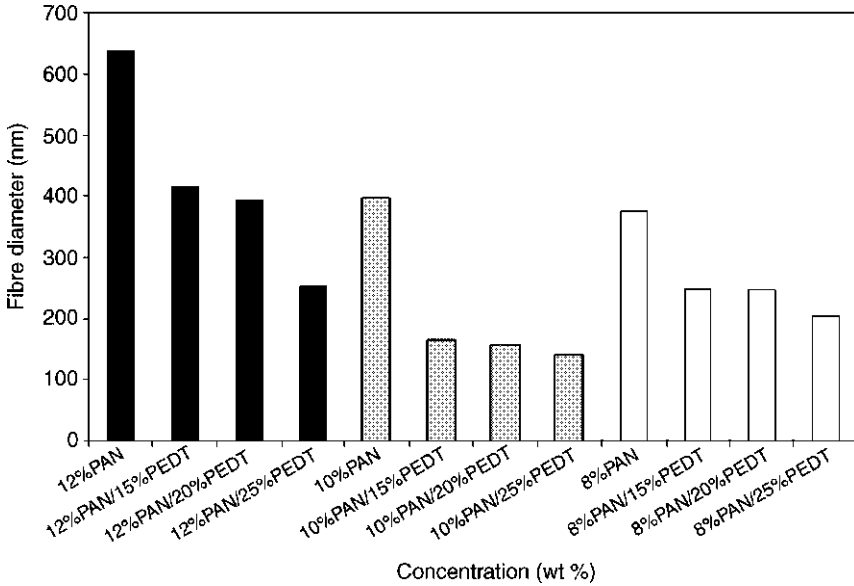
In Fig. 2.11, the diameters of the PEDT/PAN fibres are shown for various weight percent of PAN and PEDT. As expected, the diameter of the fibre decreases
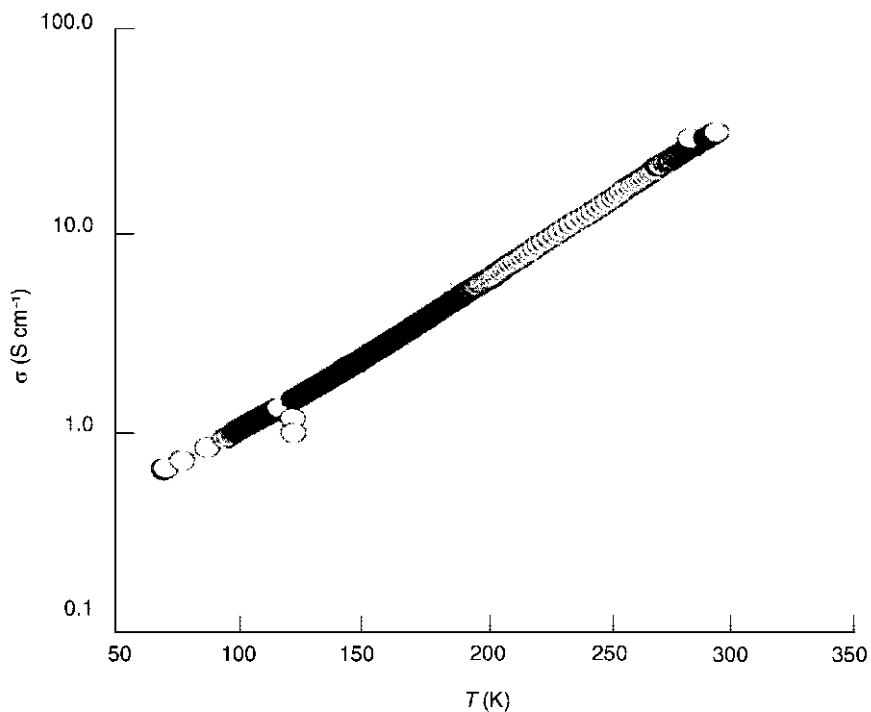
2.9 Conductivity/temperature relationship for a 72 wt% blend fibre of PANi.HCSA in PEO.
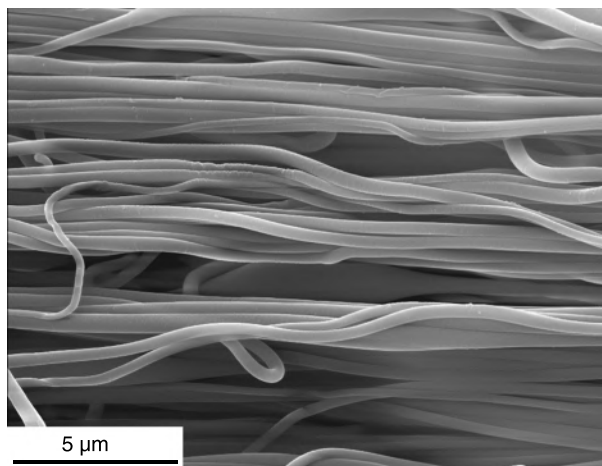
2.10 SEM image of aligned PEDT/PAN nanofibres by electrospinning.

2.11 Diameter of a fibre at various PEDT/PAN concentrations.

as the concentration of polymer-spinning dope decreases. It is of interest to note that, for the same level of PAN concentration, the addition of PEDT led to a reduction in the diameter of the fibre.

The current–voltage relationship of the PEDT/PAN fibre webs was characterised by the four-probe method. This was done by electrospinning the PEDT/PAN polymer directly on a silicon wafer. The *I/V* curves of the Si wafer with and without the fibres are shown in Fig. 2.12, from which the resistance of the wafer and wafer/fibre assemblies were calculated. By considering the Si wafer and the fibre mat to be resistors in a parallel connection, the resistance of the electrospun fibres can be calculated by applying the following relationships:

$$V = I * R$$

$$\rho = R * A / L$$

where *V* is the applied electrical potential, *I* is the current, *R* is the resistance of the material, *A* is the cross-sectional area perpendicular to the direction of the current, *L* is the distance between the two points at which the voltage is measured and ρ is the resistivity of the material (in Ω-cm). The conductivity (S cm^{-1}) of the material can be calculated from the reciprocal of the resistivity.

From Fig. 2.13, it is observed that the diameter of a fibre does indeed play an important role in the conductivity of the fibre; smaller fibres tend to have higher electrical conductivity. As shown in Fig. 2.14, the increase in the concentration of PEDT in the fibril matrix also resulted in an increase in the electrical
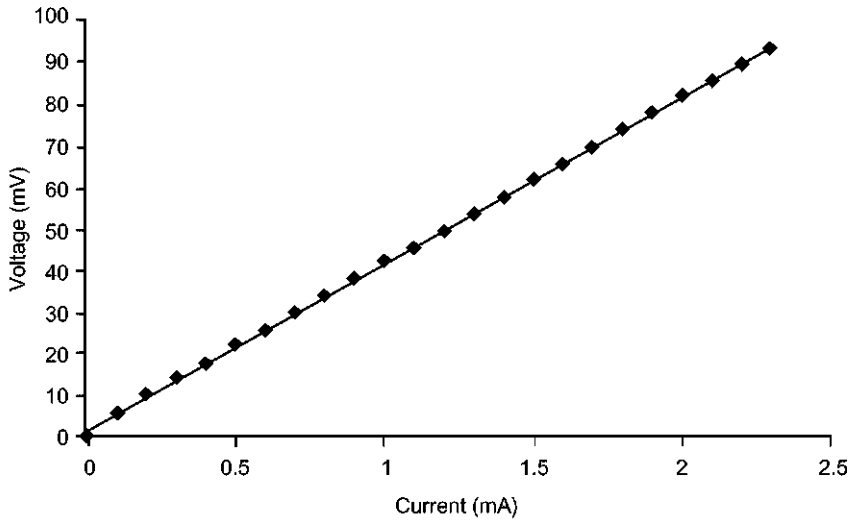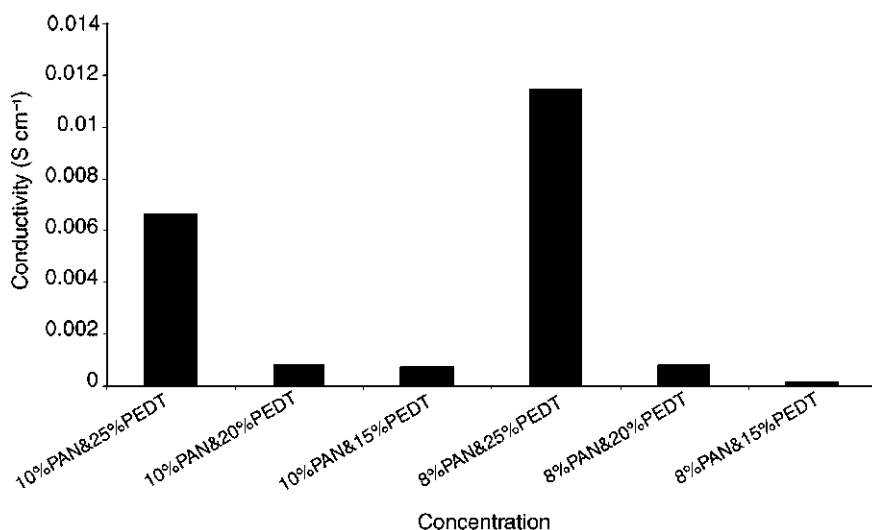
2.12 I/V curve of the PEDT/PAN nanofibre webs.
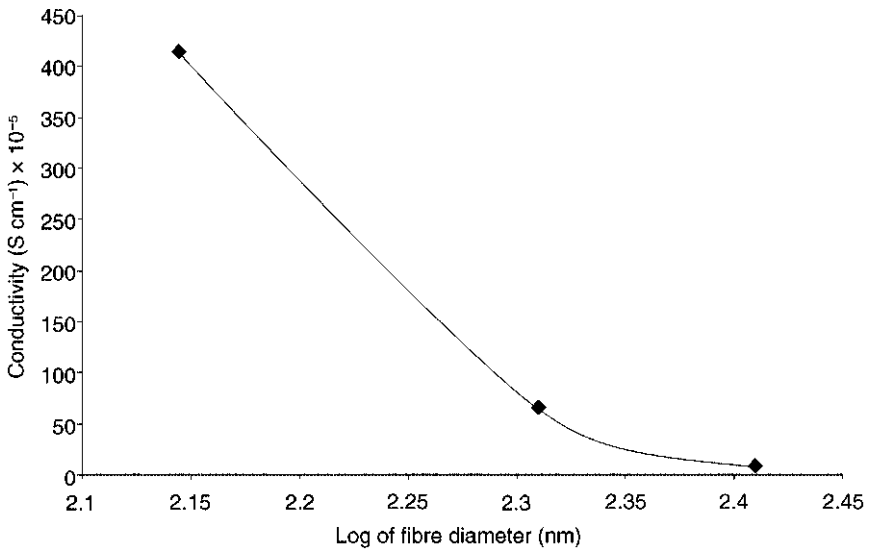
2.13 Effect of fibre diameter on electrical conductivity of PEDT/PAN fibre webs.

*2.14* Effect of concentration of PEDT on the conductivity of the fibres.

conductivity of the yarns. The measured level of electrical conductivity of the PEDT/PAN yarn was 0.001–0.012 S cm^{-1}.

2.3.2   Nanocomposites

Carbon black, metallic nanoparticles, graphite nanoplatelet and carbon nanotubes can be mixed with conductive and nanoconductive polymers to form spinning dopes for the co-electrospinning of conductive nanocomposite fibrils. Taking advantage of the high level of electrical conductivity and superior mechanical properties of carbon nanotubes,[25] the nanocomposite fibril concept will be demonstrated here using single-wall carbon nanotubes (SWNTs) as the filler.

SWNTs produced by the high pressure disproportionation of carbon monoxide (HiPco) method with an average diameter of 1.5 nm and a length of 1–2 μm were mixed in a solution of PAN/DMF to form a spinning dope for co-electrospinning. The SWNTs were magnetically stirred in the DMF for 12 h. Polyvinylpyrrolidone (PVP) was used as a surfactant to wrap the nanotubes and prevent them from re-aggregating or agglomerating. After adding the PVP to the SWNT/DMF, the suspension was sonicated for 20 min. An appropriate amount of PEDT was added to the mixture and the mixture was magnetically stirred for 15 min. Finally, a measured amount of PAN was added to the previous mixture and stirred for an additional 25 min at ~ 90°C.

The co-electrospinning of SWNT/PEDT/PAN nanofibres was successfully demonstrated with various concentrations of SWNTs, ranging from 0.2, 0.5 and 0.8 to 1 wt% in a 20 wt% PEDT/8 wt% PAN solution. To account for the increase
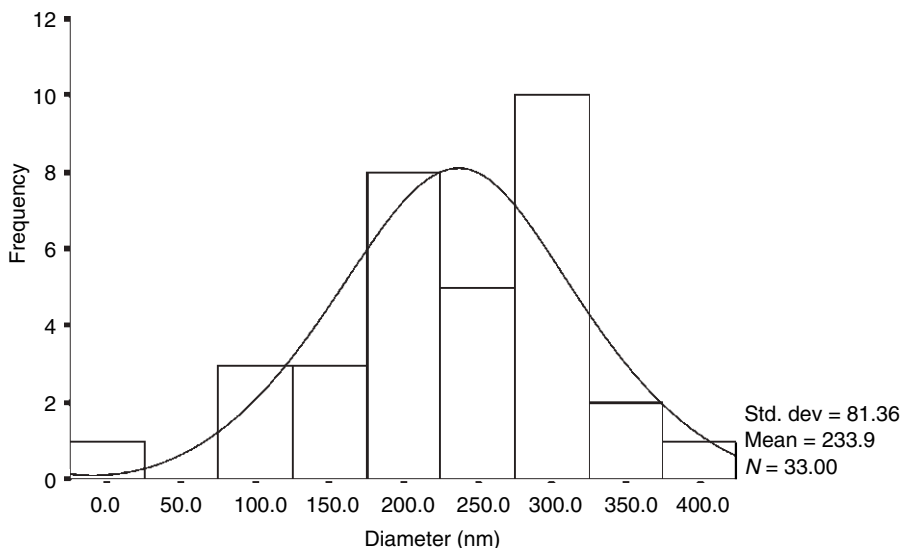
*2.15* Fibre diameter distribution of the electrospun SWNT/PEDT fibrils.

in viscosity caused by the addition of SWNTs, the concentration of polymers for the spinning dope was adjusted accordingly. Thus, for spinning dopes containing 3 and 5 wt% of SWNTs, the concentration of polymers was reduced to 10 wt% PEDT/5 wt% PAN. Figure 2.15 shows the diameter distribution of the electrospun composite nanofibres. An average fibre diameter of 230 nm was obtained from the sample.

To verify the presence of SWNT in the nanofibrils, the composite fibrils were characterised by transmission electron microscopy (TEM) and Raman spectroscopy. Figure 2.16 (a) shows the crystalline structure of the PEDT embedded in the PAN fibre with an average diameter of 200 nm. Figure 2.16 (b) illustrates the alignment of SWNT along the axis of the fibre, showing evidence that SWNT are incorporated in the nanocomposite fibrils. The diameter of the SWNT was measured to be approximately 1.2 nm, as indicated in Fig. 2.17.

The inclusion of SWNTs in the PEDT/PAN matrix fibril was further confirmed using Raman microspectroscopy (Renishaw 1000 Raman Microspectrometer) with a diode laser (780 nm excitation wavelength, 12 W cm^{-2}). Figure 2.18 shows the Raman spectra of pure PAN fibres and 0.5–1.0 wt% SWNT/PEDT/PAN fibres. The typical peaks of SWNT are the radial breathing mode (RBM) in the 100–275 cm^{-1} range, and the tangential (stretching) mode in the 1500–1600 cm^{-1} range. These peaks are evident in the SWNT/PEDT/PAN fibrils, but absent in the pristine PAN fibrils. The diameter of the SWNT can be estimated from the RBM peaks using the equation: $\omega_R \sim 224$ (cm^{-1} nm)/d, where ω_R is the RBM frequency and d is the diameter of the tube in nanometers. The presence of at least 5 RBM peaks is observed in the range from 153–267 cm^{-1}, which corresponds to diameters of tubes in the range of 0.8–1.5 nm.
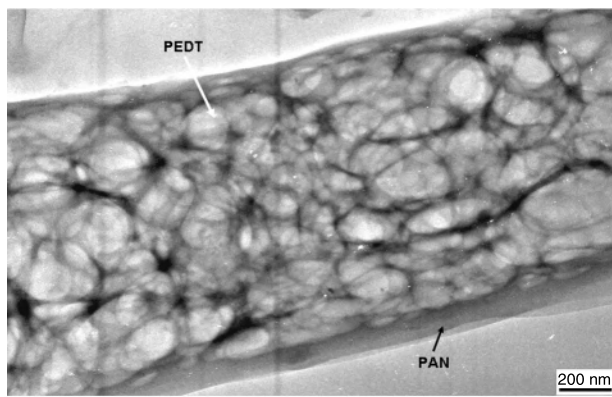
(a)
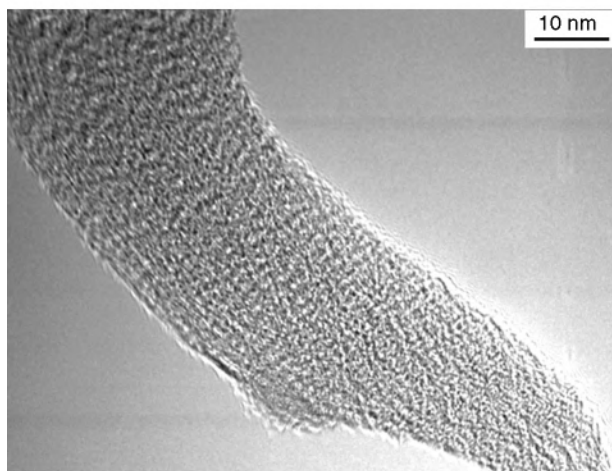
(b)

2.16 (a) TEM image of PEDT/PAN nanofibre; and (b) TEM image showing the alignment of SWNT in the PEDT/PAN nanofibres.

The electrical conductivity of the SWNT-filled nanocomposites was character-ised by the four-probe method as described in Section 2.3.1. Figure 2.19 shows that the conductivity of the fibrils increases as the weight percent of PEDT increases. The introduction of a few weight percent of SWNT leads to a significant increase in conductivity.

The effect of adding SWNTs in the PEDT/PAN matrix on the electrical conductivity of the fibrils is shown in Fig. 2.19. The presence of a few percent of SWNTs results in a doubling of the conductivity of the fibres to the level of 0.03 S cm^{-1}.
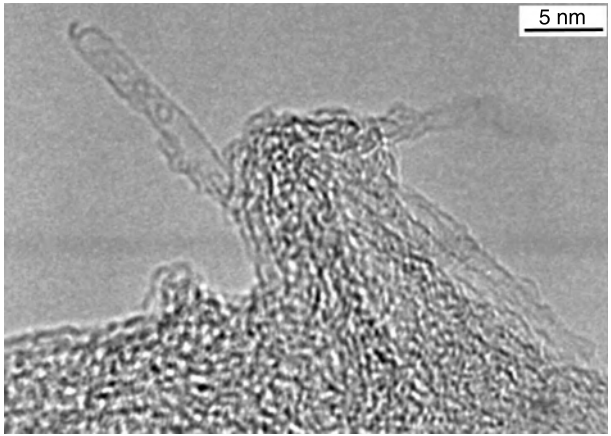
2.17 TEM image showing SWNT protruding from the fracture surfaces of the fibre.
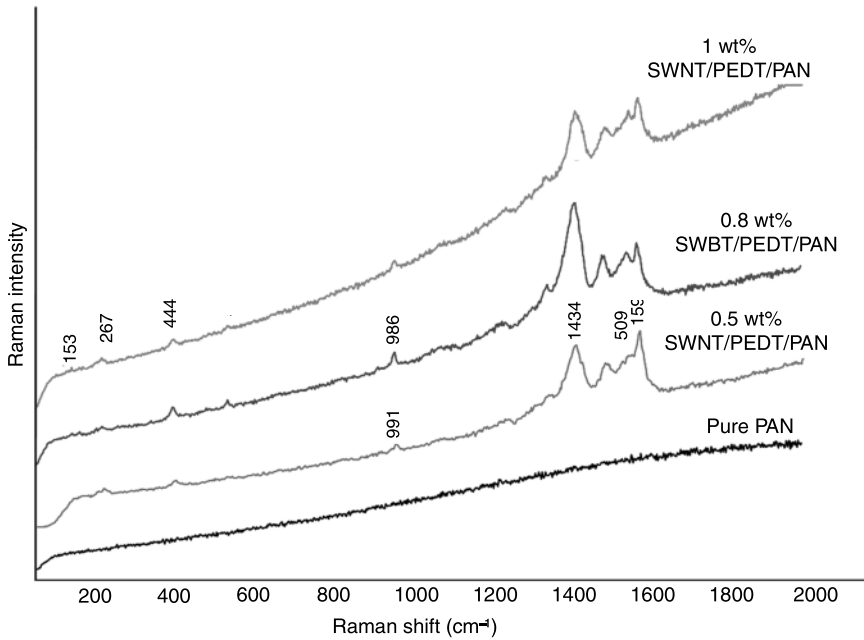
2.18 Raman spectra of composite nanofibrils of pure PAN and PEDT/PAN with various wt% of SWNTs using an excitation wavelength of 780 nm.
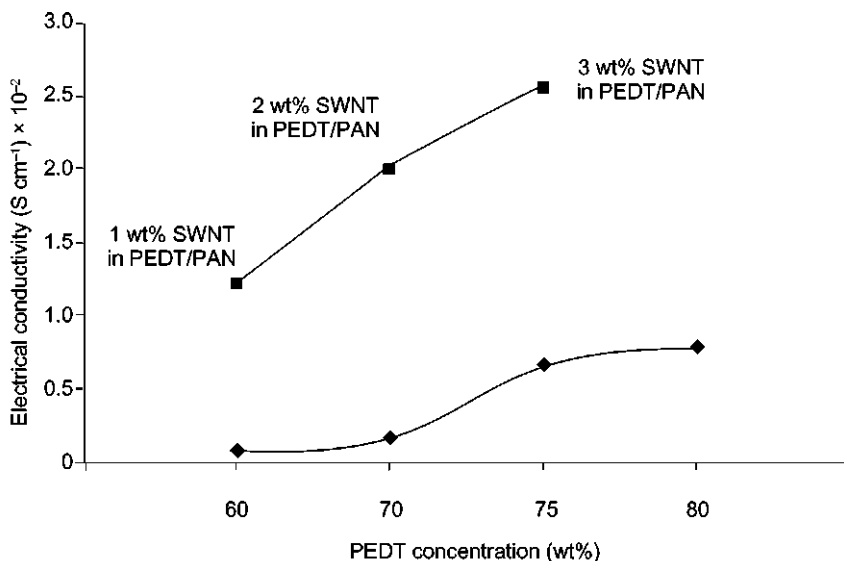
2.19 The electrical conductivity of PEDT/PAN fibrils at various levels of PEDT concentration with and without the presence of SWNTs.

2.3.3   Pyrolysis and coating of nanofibres

Electrospun fibres from organic polymers can be used as a precursor for converting to conductive nanocarbon fibres or simply used as a template for coating with a conductive polymer or metal.

Pyrolysis

As previously reported,[26] polyacrylonitrile fibres may be thermally converted to carbon nanofibres with some shrinkage. We have similarly converted a polyacrylonitrile fibre (diameter 750 nm) to a carbon fibre by first heating it in air at 200°C for 20 min, followed by heating at 800°C for 2 h under nitrogen. A current/voltage curve was obtained for a carbon fibre 600 nm in diameter. The controlled conversion of organic electrospun polymer fibres presents interesting opportunities for the fabrication of a variety of carbon nanofibres.

Electrodeless coating

The large surface-to-volume ratio offered by nanofibres makes them excellent substrates for the fabrication of coaxial nanofibres consisting of superimposed layers of different materials. Catalysts and electronically active materials can be deposited by chemical, electrochemical, solvent, chemical vapour or other means,

for use in nanoelectronic junctions and devices. It was found that polyacrylonitrile nanofibres can be easily and evenly coated with a 20–25 nm layer of conducting polypyrrole by immersion in an aqueous solution of polymerising polypyrrole.[27, 28] Analogously, we have found that the electrodeless deposition of metals can also be performed. Polyacrylonitrile fibres, for example, can be evenly coated with gold by treating them with a solution of AuS_2O_3 and ascorbic acid.

2.4   Ultra-low dielectric constant of nanocomposite fibrous film

The dielectric constant is an important electrical property of materials. It can be defined as the ratio of forces between two charges *in vacuo* to that in the medium. Alternatively, dielectric constant can be defined as the ratio of the capacity of a condenser to the capacity of the condenser *in vacuo*. The dielectric effects are the results of the polarisation of the medium between two charges when the medium is subjected to an electric field. Dielectric constant provides an indication of the relative speed that an electrical signal will travel in the medium. A medium with a low dielectric constant will result in a higher signal propagation speed since the speed of a signal is inversely proportional to the square root of the dielectric constant.[29]

Materials with a high dielectric constant are suitable for application in capacitors,[30, 31] whereas materials with a low dielectric constant are important in microelectronic and integrated circuit applications. Major advances have been made in fast and powerful microelectronic devices through miniaturisation. As the devices are getting smaller, the intermetal dielectric (IMD) constant must be low in order to reduce the resistance–capacitance (RC) time delay of the interconnects and the cross talk between metal lines. It is well known that the benefit to be derived from low-dielectric constant materials is far greater than from increasing the conductivity of the metal interconnects.

Accordingly, many laboratories are actively searching for low dielectric constant, or low K, materials. The systems that have been proposed and tested include fluorinated silica glass,[32, 33] amorphous C:F,[34] air gap formation,[35] non-fluorinated polymers,[36] inorganic–organic hybrids, porous polymer (methylsilsesquioxane), porous silica materials (Aerogel, dried by the supercritical method; or Xerogel, dried by the evaporation of solvent at ambient temperature), polyimide nanofoams,[29] Parylene-F-like film,[37] polymeric, poly(arylethers) (PAEs) (2.7–1.8, 40% porosity),[29] and fluorinated silica xerogel film.[32] In addition to low K requirement, a major challenge is to obtain materials with a low dielectric constant that have adequate mechanical strength, chemical and thermal properties, and that are capable of being integrated into manufacturing integration.

Currently, the processes being used to produce low K materials include spin casting on glass[38] and fluorinated SiO_2 ($k > 3$); nanoporous silica; crack-free

Table 2.4 State-of-the-art low K materials

Process	Structure/trade name	Manufacturer	Dielectric constant
CVD	HSQ	DOW	3.6
CVD	High K OSG	Applied Materials	3.1
CVD	Low K OSG	Applied Materials	2.7
SOD	HSQ	DOW	2.6
SOD	Porous silk	DOW	2.6
SOD	Nanoglass	Allied Signal	2.5
SOD	PTFE	Gore	2.1

Xerogel film $(1.3{\sim}2.2)$[38, 39] produced according to a law of logarithmic mixture (Lichtenecker's rule); and chemical vapour deposition (plasma-enhanced). A summary of the properties of these low K materials are shown in Table 2.4.

An examination of the state-of-the-art low K materials shows that there is a general trend to use porous materials, presumably by taking advantage of the fundamental fact that the lowest dielectric constant of one is only attainable in a vacuum. A common feature of these low K materials is that they tend to be rigid systems and many of them are brittle although they must have enough strength to endure the handling involved during processing.

We report a new class of nanofibre/nanocomposite-based ultra-low K materials produced by the electrospinning process. Through the use of ultra-fine fibres, an extremely high level of pore volume and pore surfaces can be achieved while maintaining a high level of areal coverage. The fibrous nature of the nanofibrous assembly lends itself to a flexible and conformable structure. The mechanical, chemical and thermal properties of the nanofibrous assembly can be tailored by the introduction of a second and/or third phase such as nanoparticles, nanoplatelets and nanotubes. These nanofibre and nanocomposite systems can be produced by a simple, non-mechanical process through electrostatic spinning.

To illustrate the concept of nanofibrous low K materials, PAN solutions with *N,N*,-dimethylformamide (DMF) solvent were prepared with the compositions shown in Table 2.5. The spinning solutions were prepared by mixing PAN with DMF and sonicating the mixture for 20 min. Sonication was carried out in 5-min intervals in order to keep the solution from overheating. A magnetic stirrer was used to distribute uniformly the heat generated during sonication. For the composite solution sample, the added filler was first mixed with DMF and sonicated for 20 min before being mixed with PAN to form the spinning solution, following the same procedure outlined before. Iron oxide (Fe_2O_3) nanoparticles, graphite nanoplatelets (GNP) and carbon nanotubes (CNT) were used as fillers to form nanocomposite fibres. Following the process described above, an electrostatic field of 20 kV was applied over a distance of 15 cm between the tip of the syringe needle and a 75 mm × 75 mm (3" × 3") sample ground plate covered with

Table 2.5 Composition of PAN/DMF solutions for electrospinning

DMF volume: 30 ml
PAN/DMF: 7 wt%

| DMF (g)	PAN (g)	Filler (g)	Wt% filler in PAN
26.5	1.855	0.019	1.0
26.5	1.855	0.036	2.0
26.5	1.855	0.056	3.0
26.5	1.855	0.074	4.0

Table 2.6 Dielectric constants of various nanofibrous materials measured at 100 kHz

Material	Frequency (Hz)	Dielectric constant
PAN-(A)	100k	1.46
PAN-(B)	100k	1.24
PAN-FE-1%	100k	1.16
PAN-FE-2%	100k	1.28
PAN-FE-4%-A	100k	1.14
PAN-FE-4%-B	100k	1.16
PAN-FE-8%	100k	1.08
PAN/GNP-2%-A	100k	1.18
PAN/GNP-2%-B	100k	1.16
PAN/GNP-4%-A	100k	1.07
PAN/GNP-4%-B	100k	1.15

aluminum foil. For the purposes of comparison, pristine polymer film and composite films were also prepared for subsequent characterisation of dielectric properties. A detailed description of the process has been reported elsewhere.[29]

Measurements of the dielectric constant of the nanofibrous structures were made with an Agilent 4263B LCR Meter with a 16451B Dielectric Test Fixture.[41] Electrode B of 16451B was used with a required sample diameter of between 10 and 50 mm. In order to facilitate a comparison of the test results, circular specimens were prepared with a nominal diameter of 12.5 mm. The thickness of the specimens was determined by taking an average of three measurements using a micrometer. All of the measurements were made by setting the LCR meter on a bias DC voltage of 1000 mV over the available frequency range of 1, 10 and 100 kHz. A non-contact measurement procedure or air-gap method was used for all the measurements of the dielectric constant. By measuring the capacitance of two measurements, one in which a sample was used and the other in which it was not used, this method eliminates the concern over the possible existence of gaps of
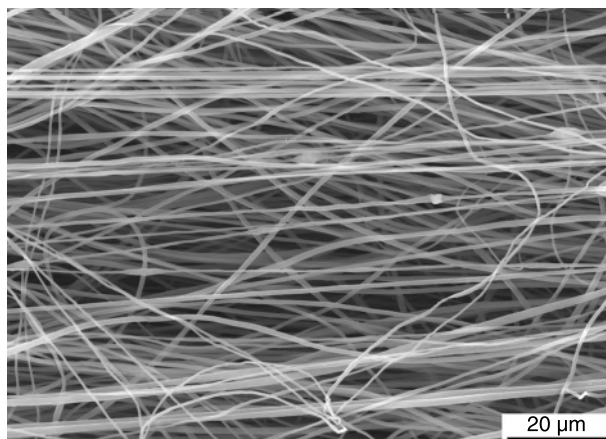
2.20 SEM image of an electrospun nanofibres mat.

air between the electrode and test sample. The dielectric constants of the nanofibrous membranes were measured at frequencies ranging from 1 to 100 kHz. The dielectric constants of various nanofibrous materials measured at 100 kHz are summarised in Table 2.6. The results show that the measured dielectric constant is between 1.1–1.46 for samples spun at 100 kHz to 20 kV. By comparison, the spun PAN has about a 39% lower dielectric constant than the cast PAN, and the composite-spun PAN has a further reduction of 12% in comparison to the spun PAN. This super-low dielectric constant associated with the nanofibrous structures may be attributed to the high level of porosity of the nanofibrous structures resulting from a tortuous three dimensional interconnected fibrous network.

The porosity of the spun fibre mats was estimated to be in the range of 70–90%. The intralayer porosity is illustrated in the SEM image shown in Fig. 2.20. This combination of high porosity, flexibility, and toughness is quite usual for nanofibrous membranes.

With further development, this family of nanofibrous materials promises to be able to meet a future demand for low K for microelectronic devices. The mechanical strength of the fibre and other requirements may be enhanced or increased by the incorporation of nanoparticles.

2.5   Conclusions

Inherently conductive polymers, polymer blends of ICP and their composites in nanofibre form and in the form of nanofibrous assemblies are promising candidates for wearable electronics. Taking advantage of the nanoscale effect, these polymer-based nanowires form the structural backbone of interconnects, functional devices, sensors, lightweight batteries for high-performance uniforms for soldiers, as well as for stylish and comfortable garments.

Electrospinning is a simple and non-mechanical process for the production of nanofibres. In order to transit this seemingly uncomplicated fibre-spinning process from a curiosity of the laboratory to a robust manufacturing process, there is a need to understand systematically the processing parameters. As a first step toward this goal, complementing ongoing electrohydrodynamic modelling,[40–46] a processing index was introduced as a means of relating the diameters of fibres to the Berry number. To convert these nanoscale fibres to clothing assemblies and integrated circuits, methods for the formation of yarn and fabric using the electrospinning process were introduced.

To demonstrate the broad range of material design concepts, the electronic properties of electrospun polyaniline, polyaniline/PEO blend, PEDT/PAN, PEDT/PAN/SWNT and PLA/SWNT were characterised. In addition, the concept of the pyrolysis of electrospun nanofibres and the use of electrospun fibres as templates for the electrodeless coating of various conducting substrates were also introduced. It was shown that one attractive feature of the ICP is the tailorability of electronic properties. The conductivity of the electrospun fibres was also shown to increase significantly with a decrease in the diameter of the fibre. It was demonstrated that ICP nanofibres are excellent candidates for ultra-sensitive sensors because of the extraordinary high surface area of the electroactive nanofibre.

The nanofibre assemblies were also shown to have unusually low dielectric constants compared to the state-of-the-art ultra low K materials. Various combinations of electrospun nanofibres with and without fillers, including PAN, PAN/CNT, PAN/Fe_2O_3 and PAN/GNP, were examined. The extremely low level of dielectric constant, less than 1.5, can be attributed to nanofibrous assemblies consisting of tortuous, interconnected networks of fibres, which are highly porous without sacrificing surface coverage. This interesting dielectric property of the nanofibrous assemblies will play an important role not only for wearable electronics, but also have significant implications for the next generation of ultra high-density integrated circuits.

Combining the advantages of low cost, control of material characteristics and design flexibility, the polymeric nanostructured fibrous assemblies are serious enabling materials for wearable electronics.

2.6   Acknowledgements

2.7   References

1. MIT Media Laboratory, http://web.media.mit.edu
2. GaTech, www.wearables.gatech.edu
3. Post R E *et al.*, *IBM System J.*, 2000, **39**, no. 3 & 4.
4. MacDiarmid A G, *Angew. Chem., Int. Ed.*, 2001, **40**.
5. Gorix Clothing Products Website, www.gorix.com
6. Kuhn H H, Child A and Kimbell W, *Synth. Met.*, 1995, **71**.
7. Nabet B, 'When is small good? On unusual electronic properties of nanowires', ECE Department, Philadelphia, PA-19104.
8. Yao Z *et al.*, *Nature*, 1999, **402**, 6759.
9. Hulteen J C and Martin C R, *J. Mater. Chem.*, 1997, **7**(7).
10. Hongu T and Phillips G O, *New Fibers*, 1997.
11. Formhals A, U.S. Patent # 1,975,504, 1934.
12. Doshi J and Reneker D H, *J. Electrostatics*, 1995, **35**, 151.
13. Gibson P W, Schreuder-Gibson H L and Riven D, *AIChE J.*, 1999, **45**, 190.
14. Ko F K, Laurencin C T, Borden M D and Reneker D H, 'The dynamics of cell-fiber architecture interaction', in *Proceedings, Annual Meeting, Biomaterials Research Society*, San Diego, April 1998.
15. Reneker D H and Chun I, *Nanotechnology*, 1996, **7**(3), 216.
16. Baumgarten P K, *J. Colloid Interface Sci.*, 1971, **36**(1).
17. Sachiko S, Gandhi M, Ayutsede J, Micklus M and Ko F, *Polymer*, 2003, **44**, 5721–5727.
18. Hager B L and Berry G C, *J. Polymer Sci., Polym. Phys. Edn*, 1982, **20**, 911.
19. Norris I D, Shaker M M, Ko F K and MacDiarmid A G, *Synth. Met.*, 2000, **114**(2), 109.
20. ASTM Designation: D4496-87-453.
21. Iijima S, *Nature*, 1991, **354**, 56.
22. Xia Y, MacDiarmid A G and Epstein A J, *Macromolecules*, 1994, **27**, 7212.
23. MacDiarmid A G, Min Y, Wiesinger J M, Oh E J, Scherr E M and Epstein A J, *Synth. Met.*, 1993, **55**, 753.
24. El-Aufy A, Preprint submitted to the *226th American Chemical Society National Meeting*, New York, NY, September 7–13, 2003.
25. Saito R, Dresselhaus G and Dresselhsaus M S, *Physical Properties of Carbon Nanotubes*, 1998.
26. Chun I, Reneker D H, Fong H, Fang X, Deitzel J, Tan N B and Kearns K, *J. Adv. Mater.*, 1999, **31**(36).
27. Huang Z, Wang P C, MacDiarmid A G, Xia Y and Whitesides G M, *Langmuir*, 1997, **13**(6480).
28. Gregory R V, Kimbrell W C and Kuhn H H, *Synth. Met.*, 1989, **28**(1–2), C823.
29. Luoh R, Ko F K and Hahn H T, *Proceeding of the 14th International Conference on Composite Materials* (ICCM-14), July 14–18, 2003, San Diego, CA.
30. http://www.mtiinstruments.com/gaging/appnotes-aci_doc.html
31. http://www.ece.gatech.edu/research/labs/vc/packaging/lectures/lecture5.pdf
32. Pai C S, Velaga A N, Lindenberger W S, Lai W Y, Cheung K P, Bauman F H, Chang C P, Liu C T, Liu R, Diodato P W, Colonell J I, Vaidya H, Vitkavage S C, Clemens J T and Tsubokur F, Interconnect Technology Conference, 1998. *Proceedings of the IEEE 1998 International*, June 1998, pp 39–41.
33. Xu Y, Tsai Y, Tu K N, Zhao B, Liu Q, Brongo M, Sheng G and Tung C H, *Appl. Phys. Lett.*, 1999, **75**(6).
34. Chang K M, Yang J and Chen L, *IEEE Electron Device Letters*, 1999, **20**(4).

35. He L and Xu J, *Proceedings of the 6th International Conference on Solid-State and Integrated-Circuit Technology*, 2001, **1**.
36. Gorman B, Orozco-Teran R, Roepsch J, Dong H, Reidy R and Mueller D, *Appl. Phys. Lett.*, 2001, **79**(24).
37. Hanyaloglu B, Aydinli A, Oye M and Aydi E, *Appl. Phys. Lett.*, 1999, **74**(4).
38. http://domino.research.ibm.com/tchjr/journalindex
39. Purushothaman S *et al.*, Electron Devices Meeting, *2001 IEDM Technical Digest*, 2001.
40. Doshi J and Reneker D, *J. Electrostatics*, 1995, **35**.
41. Kazuhiko E and Tatsumi T, *J. Appl. Phys.,* 1995, **78**(2).
42. Yan F, Farouk B and Ko F K, 'Numerical modeling of an electrostatically driven liquid meniscus in the cone-jet mode', *Aerosol Sci.*, 2003, **34**, 99–116.
43. Fridrikh S V, Yu J H, Brenner M P and Rutledge G C, 'Electrostatic production of nanofibers: control of the fiber diameter', *Proceeding of the 6th International Conference on Textile Composites* (TEXCOMP-6), September 11–13, 2002, Philadelphia, PA.
44. Dror Y, Salalha W, Khalfin R L, Cohen Y, Yarin A L and Zussman E, *Langmuir*, 2003, **29**.
45. Spivak S F, Dzenis Y A and Reneker D H, *Mechanics Res. Commun.*, 2000, **27**(1).
46. Storr G J and Behnia M, *Exp. Therm. Fluid Sci.*, 2000, **22**.